Jurnal Pertahanan

Media Informasi tentang Kajian dan Strategi Pertahanan
yang Mengedepankan *Identity*, *Nationalism* dan *Integrity*
e-ISSN: 2549-9459
http://jurnal.idu.ac.id/index.php/DefenseJournal

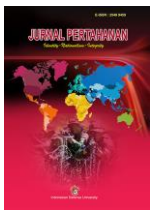

SYNTHESIS AND CHARACTERIZATION OF $CoTi_{(1-X)}Mn_{(X)}O_3$ AS A RADAR ABSORBING MATERIAL

Maspin Apit
Faculty of Defense Technology, Indonesia Defense University
IPSC Area, Sentul, Sukahati, Citeureup, Bogor, West Java, Indonesia 16810
maspinapit@gmail.com

Romie Oktovianus Bura
Faculty of Defense Technology, Indonesia Defense University
IPSC Area, Sentul, Sukahati, Citeureup, Bogor, West Java, Indonesia 16810
romiebura@idu.ac.id

Wisnu Ari Adi
Science and Technology of Advanced Materials, National Nuclear Energy Agency of Indonesia
Gedung 42, Jl. Kawasan. Puspiptek, Muncul, Setu, Tangerang Selatan, Banten, Indonesia 15314
dwisnuaa@batan.go.id

R. Andhika Ajiesastra
Research & Development Agency, Ministry of Defense of Republic of Indonesia
Jl. Jati No. 1 Pondok Labu, Jakarta Selatan, Jakarta, Indonesia 12450
andika.ajie.sastra@kemhan.go.id

Article Info

Article history:
Received 14 January 2020
Revised 9 March 2020
Accepted 26 March 2020

Keywords:
Anti Radar,
$CoTiO_3$,
Electromagnetic wave absorption,
Mn,
Mechanical Milling

DOI:
http://dx.doi.org/10.33172/jp.v6i1.697

Abstract

To avoid detection from Radio Detection and Ranging (Radar), one of the efforts is to use Radar absorbing material. One of the Radar wave absorbing materials is Perovskite $CoTiO_3$. This Paper investigated the ability of $CoTi_{(1-x)}Mn_{(x)}O_3$ to absorb the Radar wave. $CoTi_{(1-x)}Mn_{(x)}O_3$ with variations x = 0, 0.01, 0.02, and 0.03 have been successfully synthesized using the mechanical milling method. The XRD pattern shows that the sample formed was single phase $CoTiO_3$. Surface morphology resulting from measurements with SEM shows homogeneous particles and an average size of 200 nm. The results of measurements with VNA at X-band frequency (8.20 GHz - 12.4 GHz) show that the absorption ability of electromagnetic waves from $CoTiO_3$ increases with the increase in doping from Mn^{4+}. Maximum results obtained at the composition x=0.03 ($CoTi_{0.97}Mn_{0.03}O_3$) with a reflection loss (RL) value is -14.56 dB (%Abs is 81.3%) at a frequency of 9.96 GHz. This result proves that $CoTi_{(1-x)}Mn_{(x)}O_3$ can be used as a Radar absorbing material at X-band frequency.

INTRODUCTION

Several countries in the world utilize Radar technology for military purposes both in defense and during attacks (Wang, Hu, Zhang, Gao, & Cai, 2018). Radar is used to detect, measure the distance, speed and direction of an object approaching an area equipped with Radar (Keerthana, Shanmugha Sundaram, & Soman, 2018). Combat aircraft, missiles, ships, satellites and tanks and other land vehicles use Radar technology to detect the presence of enemies (Shiva, Elleithy, & Abdelfattah, 2017). So it is difficult to attack units or areas equipped with the Radar system. To avoid detection from Radar, one of the efforts is to use Radar absorbing material (Lee, Choi, & Lee, 2015).

The use of Radar absorbing material can significantly increase the survivability of a military device in modern warfare (W. Li, Lina, Lia, Wang, & Zhang, 2019). To develop Radar absorbing material, the conditions that must be met by a material is that it must have high permeability and permittivity (Lenin, Sakthipandi, Kanna, & Rajesh, 2018). Perovskite $CoTiO_3$ has high permittivity (Silva, Oliveira, Silva, & Sombra, 2019) but low permeability (Schoofs, Egilmez, Fix, MacManus-Driscoll, & Blamire, 2013). Mn^{4+} can improve the permeability of perovskite (Phan et al., 2012). Therefore, to improve the ability of $CoTiO_3$ to absorb Radar waves, this research was conducted Mn doping on $CoTiO_3$.

This study aims to analyze whether the mechanical milling method can produce single phase $CoTiO_3$ doping Mn compounds. Based on the theory above, it is expected that Mn doping can increase the absorption ability of Radar waves from $CoTiO_3$.

THEORETICAL FRAMEWORK

Electromagnetic wave

Electromagnetic waves are transverse oscillations of interconnected electric and magnetic fields that travel through space, through empty space, they move at the speed of light in vacuum, through other media, their speed is reduced by the refractive index value of the medium.

Electromagnetic spectrum is defined as a graphical representation of electromagnetic waves arranged according to their wavelength. The types of electromagnetic spectrum are radio waves, microwaves, infrared, visible light, ultraviolet, X-rays, and gamma rays (Zwinkels, 2015). Electromagnetic waves are a form of energy that is emitted and absorbed by charged particles, which shows wave-like behavior as it moves through space. Electromagnetic energy propagates in waves with several parameters that can be measured, namely, wavelength, frequency, amplitude,

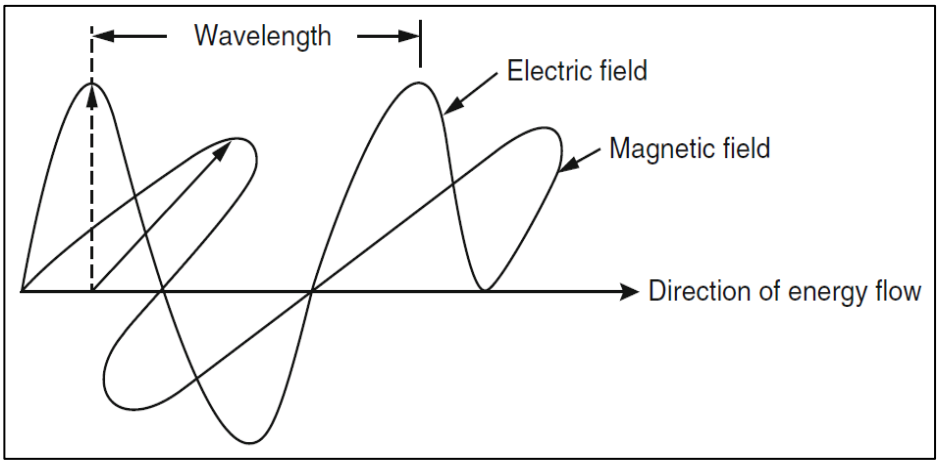

Figure 1. Electromagnetic Wave
Source: Zwinkels, 2015

and speed (Adi et al., 2019).

Radio Detection and Ranging (Radar)

Radar, which stands for "Radio detection and ranging", shows a system that uses reflected radio frequency energy to detect and locate objects, measure distance or altitude, navigation, bombing and other purposes (Lee et al., 2015). Radar was first investigated by Heinrich Hertz at the end of the 19th century. Hertz said that radio waves are reflected by metal objects. Motivated by James Clerk Maxwell's study of electromagnetic waves, Hertz demonstrated the reflection of these waves with metal objects. In 1887, Hertz experimented further with electromagnetic waves and discovered that some waves could be transmitted through several materials while others reflected these waves back to their source (Emery, W & Camps, 2017).

Advances in Radar systems have enabled the system to detect, differentiate, classify interest targets, and measure distance, speed, and direction of travel (Keerthana et al., 2018). Given Radar's wide application in the military, its effectiveness is directly related to the strength of various weapons and equipment, surveillance and warning, placement, connection, command and control of various coordinated weapons operations. The Radar confrontation for a long time, always dominated electronic warfare (Wang et al., 2018).

Observation and detection in a Radar system is mainly influenced by unwanted reflections from the land and sea level. This reflection is generally referred to as chaos. The echo signal collected from the target consists not only of target information but also messy informa tion (X. M. Li, Luo, Qiu, & Li, 2011). Starting from the beginning of the 20th century, Radar has often been used in a number of different applications, for example, military navigation, space and air navigation, air traffic control, and ship safety (Emery, W & Camps, 2017).

The Radar system is used on aircraft, missiles, satellites, ships and land vehicles. The Radar system is fundamentally classified into two broad configurations based on the spatial overlap between the transmitting and receiving antennas: they are monostatic and bistatic types. The use of two antennas in bistatic Radar makes the design of Radar systems complex and high cost. The line of sight is needed because of the low spatial level coverage in the case of bistatic Radar. Monostatic Radar can provide a cost-effective design good spatial coverage and better target

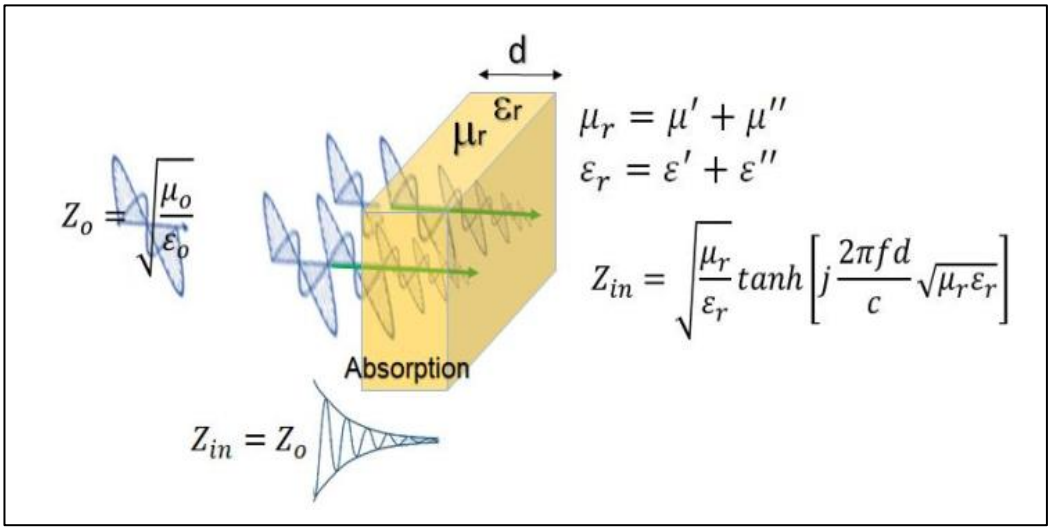

Figure 2. Radar Wave Absorption Mechanisms
Source: Adi et al., 2019

tracking and detection capabilities, along with estimation of target positions (Sai (Shiva et al., 2017).

Radar Wave Absorption Mechanisms

Coherent and polarized Radar waves obey optical laws, ie waves can be reflected, transmitted, and absorbed, depending on the type of material through which they pass. In general, the use of Radar waves is based on its utilization on the phenomenon of reflection and transmission only. But in the last few decades, the phenomenon of absorption of Radar waves has been used for the development of rapidly developing telecommunications, electronic and defense technologies (Liu et al., 2004). The main requirement needed as a material for absorbing Radar waves is that this material has permeability (magnetic loss) and permittivity (dielectric loss) value (Wu et al., 2018).

It is known that dielectric and magnetic parameters include electric field vector, magnetic field, induction field, displacement, polarization, and magnetization (Folgueras, Alves, & Rezende, 2010). The interaction of an electric field in a material follows a pattern similar to the magnetic interaction in a material. One of the requirements that must be met for practical applications as electromagnetic wave absorbers is that this material must have high permeability and permittivity values with high magnetic saturation. Permitivity in farads per meter and permeability in henries per meter. In the case of absorption of electromagnetic wave energy, the overall interaction can be represented by matching the dielectric and magnetic impedance of the material (Z_{in}) which is the same as the air impedance (Z_o) as a function of frequency (Adi et al., 2019).

This impedance adjustment is important in the radar wave frequency range. Matching means providing the same impedance as the characteristic impedance of electromagnetic waves. The parameter measured is reflection loss (RL), if there is a matching impedance $Z_{in} = Z_o$, meaning that RL will become infinite or all waves have been absorbed perfectly (Adi et al., 2019).

Radar Wave Absorber Material

The main requirement needed as a material for absorbing Radar waves is that this material has permeability (magnetic loss) and permittivity (dielectric loss) value (Wu et al., 2018). Radar wave absorbing material has generated great interest among researchers since the discovery of the Radar system used by the military to identify defense-based objects. The X-band (8-12 GHz) Radar system is well known in the defense sector because of its high resolution imaging and greater precision target identification. Since World War II, Radar wave absorbing materials have given much attention to researchers because of their unique and promising applications in the field of aircraft technology, warships, tanks and missiles by making them invisible to Radar (Panwar, Agarwala, & Singh, 2015). Radar wave absorbing materials can significantly increase the ability to survive and penetrate military hardware that is widely used in modern warfare by reducing Radar detection. However, when Radar detection technology was developed, the demand for Radar absorbing materials continued to increase (W. Li et al., 2019).

$CoTiO_3$ doping Mn

One of the ingredients selected in this study is the ingredient Perovskite-based magnetic $CoTiO_3$. $CoTiO_3$ is a dielectric material and is used successfully for random access memory cell capacitors. Because of its high dielectric permittivity, it has an advantage in the field of semiconductor devices. $CoTiO_3$ has been proven as a stable material at high temperatures. $CoTiO_3$ has also been used successfully in gas sensors for ethanol, magnetic recorders and photocatalysts (Silva et al., 2019). $CoTiO_3$ is a semiconductor material with a Nel

temperature of around 38 K (R. E. Newnham, 1964) and a band gap of 2.53 eV. (M. W. Li, Gao, Hou, & Wang, 2013). $CoTiO_3$ has high dielectric properties (Schoofs et al., 2013) on the other hand, $CoTiO_3$ is used in applications such as humidity (He., 2007) and gas sensors (Siemons & Simon, 2007).

Many studies on $CoTiO_3$ such as, Chu *et al*, (Chu et al., 1999) show that $CoTiO_3$ nano powder with increased surface area is a good material for ethanol sensing applications. Sarkar *et al*, (Sarkar et al., 2014) synthesized the $CoTiO_3/TiO_2$ heterostructure used in cyclohexane oxidative dehydrogenation with good conversion efficiency and benzene selectivity. Cheng-Gao Sun *et al*, (C. G. Sun et al., 2006) reported mesoporous Co-Ti oxide material with a specific surface area of 204 m^2/g. Guorui Yang *et al*, (Yang, Yan, Wang, & Yang, 2014) reported interesting materials such as $CoTiO_3$ nanofibers with a specific surface area of 20 m^2/g. (Vinogradov, Vinogradov, Gerasimova, & Agafonov, 2012) successfully synthesized $CoTiO_3$ crystalline layers at low temperatures. B. C. Yadav *et al*, (Yadav et al., 2013) reported the nanostructured $CoTiO_3$ film for humidity sensing applications with an average crystal size of 21.5 nm. $CoTiO_3$ has green pigment (Zou & Zheng, 2016).

Perovskite $CoTiO_3$ has high permittivity (Silva et al., 2019) but low permeability (Schoofs et al., 2013). Mn^{4+} can increase Perovskite permeability (Phan et al., 2012). Phan *et al*, (Phan et al., 2012) in their research explained that Mn^{4+} can improve the permeability of Perovskite. Increasing the permeability can increase the ability of Radar absorption of a material (Lenin et al., 2018). Therefore, in this study Mn^{4+} doping on CoTiO3 was used to increase the ability of $CoTiO_3$ to absorb Radar waves.

METHODS

Preparation of $CoTi_{(1-x)}Mn_{(x)}O_3$

Research approach used in this study is quantitative with synthesis method is mechanical milling. This method is very flexible, easy to do and controlled by various parameters needed such as grinding material, the ratio of ball weight to material, speed of movement, and speed of grinding and can be used to avoid unnecessary chemical reactions. In addition, further engineering optimization and repair costs have made this technique feasible for industry, and various materials are currently needed on an industrial scale (Khalil & Celik, 2019).

Co_3O_4, TiO_4, MnO_4 were weighed according to the stoichiometric calculations of each variation x = 0, 0.01, 0.02, and 0.03, four sample is enough (Gunanto, Jobiliong, & Adi, 2016). After that, put into vials, each compound put in vials and ball mills with a mass ratio of 1: 1, where the weight of each ingredient in vials of 5 grams and ball mills put into 5 pieces (1 piece of ball mill weighs 4 grams) so that the total mass of iron balls is 20 grams. Then given the addition of ethanol 2/3 by volume vial. This process is called wet milling. After that the vial is inserted into the mechanical milling device.

The milling process is carried out for 5 hours. After the milling process is completed, the vial is released from the mechanical milling device and the vial lid is opened then the drying process is carried out with an oven at 100^{o}C for 5 hours. Then it was sintered at 1000^{o}C for 5 hours. The Preparation of this material was done in Science And Technology Of Advanced Materials, National Nuclear Energy Agency Of Indonesia Laboratory.

Characterization

Each phase of the synthesized powder was

carried out by phase identification with XRD. Surface morphology and composition with SEM-EDS. The measurements was done in Science And Technology Of Advanced Materials, National Nuclear Energy Agency Of Indonesia Laboratory. Measurement of Radar wave absorption with VNA. This measurement was done in Research & Development Agency Ministry of Defense Indonesia

RESULT AND DISCUSSION

Figure 3, a sample of $CoTi_{(1-x)}Mn_{(x)}O_3$ synthesized using the mechanical milling method. The sample is in the form of a green powder which is a characteristic color of $CoTiO_3$. The color of $CoTiO_3$ does not change even though it has been doped with Mn^{4+} elements, it is proven that $CoTi_{(1-x)}Mn_{(x)}O_3$ samples start from $CoTiO_3$ (x = 0), $CoTi_{0.99}Mn_{0.01}O_3$ (x = 0.01), $CoTi_{0.98}Mn_{0.02}O_3$ (x = 0.02), and $CoTi_{0.97}Mn_{0.03}O_3$ (x = 0.03) which is a Mn^{4+} doped $CoTiO_3$ sample remains green like x = 0 which is $CoTiO_3$ without Mn^{4+} doping. With the green pigment $CoTiO_3$ suitable to be used as a material for absorbing Radar waves for military purposes, because the green pigment can be applied to the identity and color code of camouflage for Indonesia, which has a green environment. In physics, colors are created from reflected light waveSs that are not absorbed by pigments. In this study, the colors appear green and have wavelengths between 480-560 nm (Zwinkels, 2015). The discoloration occurs along with giving the right temperature at the time of sintering.

Figure 3. $CoTi_{(1-x)}Mn_{(x)}O_3$ Powder
Source: The Authors, 2020

Phase identification of the sample was carried out using the X-Ray Difraction (XRD) brand PAN Analytical Empyrean Anode Cu Kα Wavelength 1.5406 Å. Figure 4 shows the results with XRD measurements showing a single phase for all $CoTi_{(1-x)}Mn_{(x)}O_3$ samples starting from x = 0, 0.01, 0.02, and 0.03. The diffraction pattern formed indicates an indication of the formation of the $CoTiO_3$ phase with its main peak at 2θ around the 32.8° angle which is the plane peak of the $CoTiO_3$ which is supported by other peaks at an angle of 24.1°, 35.45°, 40.57°, 49.11°, 53.54°, 61.9°, and 63.61°, which is in accordance with the data in COD (Crystallography Open Database) number 2310633. The single phase produced for all of these samples proves that the Mn^{4+} ion substitution was successfully carried out into the $CoTiO_3$ structure by not changing the crystal structure of $CoTiO_3$ itself.

Figure 5 shows the results of quantitative analysis of X-ray diffraction patterns of $CoTi_{(1-x)}Mn_{(x)}O_3$ samples starting from x = 0, 0.01, 0.02, and 0.03. Figure 5 (a-d) is the result of an improvement in the XRD pattern for x = 0, 0.01, 0.02, and 0.03 which has formed a single phase diffraction peak. This quantitative analysis refers to crystallographic data from an open database with COD (Crystallography Open Database) number 2310633 for the $CoTiO_3$ phase.

The results of the improvement of X-ray diffraction patterns in Figure 5 and Table 1 have excellent refinement quality in accordance with the criteria of fit (Rwp) and goodness of fit ($\chi 2$) (Kumar, Supriya, Pradhan, & Kar, 2017). The Rwp statistical parameter is the weight ratio of the difference between the observation pattern and the XRD pattern calculation

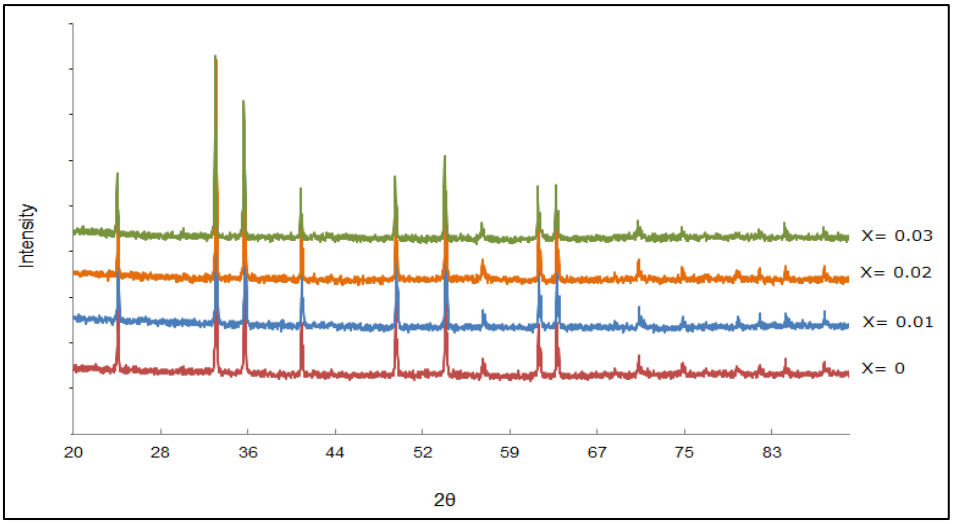

Figure 4. XRD Pattern of $CoTi_{(1-x)}Mn_{(x)}O_3$
Source: Processed by Authors, 2020

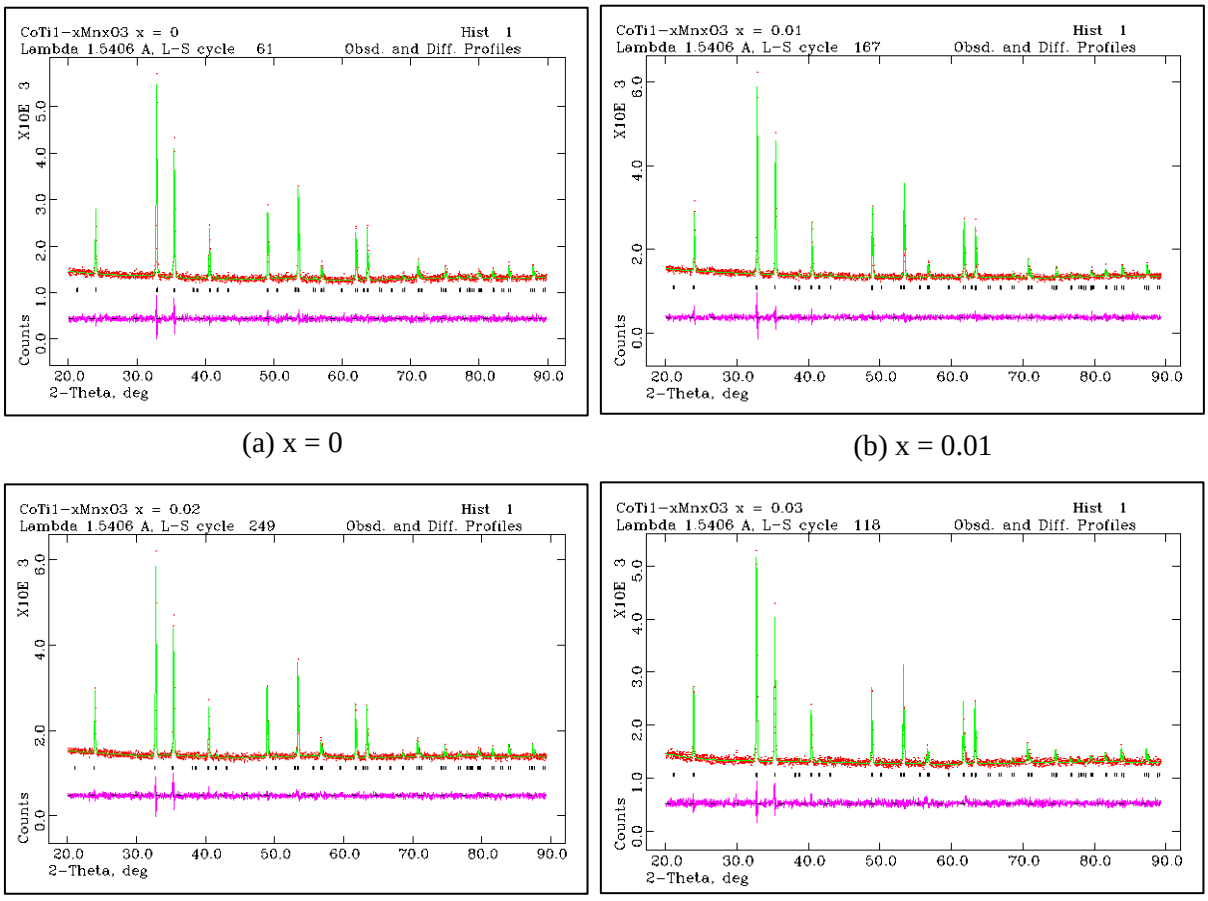

(a) x = 0 (b) x = 0.01

(c) x = 0.02 (d) x = 0.03

Figure 5. Refinement Results of $CoTi_{(1-x)}Mn_{(x)}O_3$
Source: GSAS Software processed by Authors, 2020

where the best value is <10%, while the statistical parameter $\chi 2$ (chi-square) is the ratio of the comparison of the calculation pattern and XRD expectation. calculations where the best value is $1 < \chi 2 < 1.3$ (Akmal Johan, Wisnu Ari Adi, 2019).

Table 1. The Criteria of fit (Rwp) and goodness of fit ($\chi 2$) of Each Sample $CoTi_{(1-x)}Mn_{(x)}O_3$

X	Rwp (%)	χ^2
0	3.05	1.280
0.01	2.98	1.271
0.02	3.02	1.331
0.03	3.10	1.313

Source: GSAS Software processed by Authors, 2020

The surface morphology and composition of $CoTi_{(1-x)}Mn_{(x)}O_3$ powder were seen using SEM (Scanning Electron Microscope) brand JEOL type JED 2300. Figure 6 shows the results of SEM measurements of 5000x magnification of visible particles homogeneous and the average particle size $CoTi_{(1-x)}Mn_{(x)}O_3$ is at 200 nm.

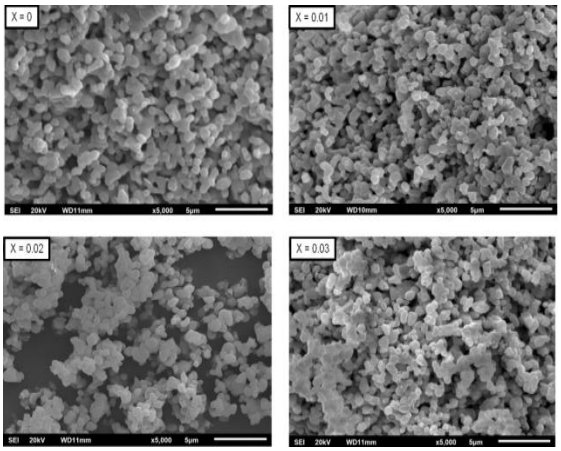

Figure 6. Surface Morphology of Powder $CoTi_{(1-x)}Mn_{(x)}O_3$
Source: Processed by Authors, 2020

The relationship between reflection loss (RL) with the frequency of $CoTi_{(1-x)}Mn_{(x)}O_3$ powder can be seen in figure 7. Absorption of Radar waves is done at X-band frequency 8.2 - 12.4 ghz, measurement using a vector network analyzer (VNA) brand keysight n5232a pna-l network analyzer 300 khz - 20 ghz. It can be seen from the picture that the increased absorption ability of Radar waves by $CoTi_{(1-x)}Mn_{(x)}O_3$ samples increases with the increasing number of Mn^{4+} doping ion.

Table 2. The Maximum and Average RL Value of Each Sample $CoTi_{(1-x)}Mn_{(x)}O_3$

X	RL max (dB)	Frequency (GHz)	Average RL (dB)
0	-7.93	8.87	-4.75
0.01	-12.25	9.96	-5.30
0.02	-12.34	10.47	-7.00
0.03	-14.56	9.96	-5.91

Source: Processed by Authors, 2020

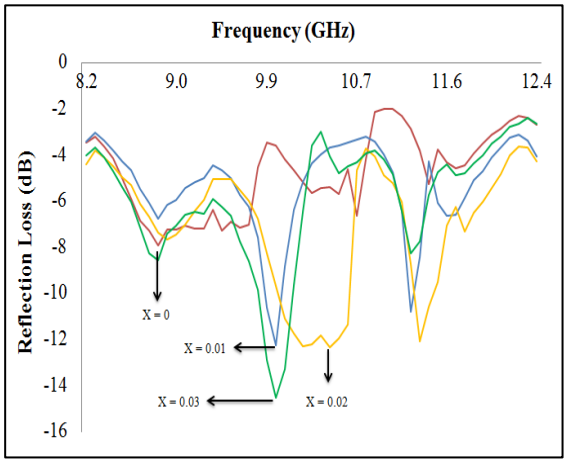

Figure 7. Reflection Loss (RL) from $CoTi_{(1-x)}Mn_{(x)}O_3$ Powder at X-Band Frequency (8.2 - 12.4 Ghz)
Source: Processed by Authors, 2020

Table 2 shows the maximum and average RL of each sample. Maximum RL value of each sample increases with the increasing number of Mn^{4+} doping ion. Maximum results were obtained for doped ion Mn^{4+} x = 0.3 ($CoTi_{0.97}Mn_{0.03}O_3$), where the maximum RL value is -14.56 dB at a frequency of 9.96 GHz. The maximum average results were obtained for doped ion Mn^{4+} x = 0.2 ($CoTi_{0.98}Mn_{0.02}O_3$), where the value is -7.00 dB.

The relationship of maximum RL values with the ability of Radar wave absorption or %absorption (%abs) can be calculated using equation (1) as follows:

$$RL = (20)\ \text{Log}\ \frac{100\text{-}\%Abs}{100} \quad (1)$$

In Figure 8 it can be seen that %abs $CoTi_{(1-x)}Mn_{(x)}O_3$ in absorbing Radar waves increases with the addition of Mn^{4+}. Where for variation x = 0 (RL max -7.93 dB at 8.87 GHz frequency) has a %abs 59.9%, variation x = 0.01 (RL max -12.25 dB at frequency 9.96 GHz) has %abs 75.6%, variation x = 0.02 (RL max -12.34 dB at a frequency of 10.47 GHz) has a %abs 75.9%, and variations of x = 0.03 (RL max -14.56 dB at a frequency of 9.96 GHz) has a %abs 81.3%.

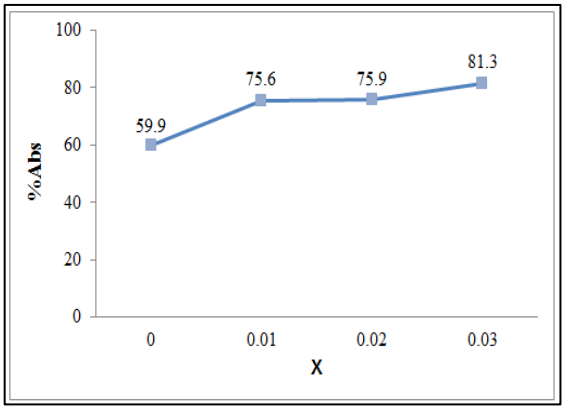

Figure 8. %Abs of $CoTi_{(1-x)}Mn_{(x)}O_3$
Source: Processed by Authors, 2020

CONCLUSIONS

$CoTi_{(1-x)}Mn_{(x)}$ was successfully synthesized using the Mechanical Milling method. The addition of Mn^{4+} ions can increase the ability to absorb Radar waves from $CoTiO_3$. Maximum results were obtained for Mn^{4+} x = 0.03 ($CoTi_{0.97}Mn_{0.03}O_3$) doping ion with a maximum RL value of -14.56 dB (% Abs = 81.3%) at a frequency of 9.96 GHz. This result proves that $CoTi_{(1-x)}Mn_{(x)}O_3$ can be used as an Radar absorbing material at X-band frequency.

ACKNOWLEDGMENTS

On this occasion the authors would like to say thanks to Indonesia Defense University, Science And Technology Of Advanced Materials, National Nuclear Energy Agency Of Indonesia, Serpong, Indonesia and Research & Development Agency Ministry of Defense, Jakarta, Indonesia which funded and facilitated this research.

REFERENCES

Adi, W. A., Yunasfi, Y., Mashadi, M., Winatapura, D. S., Mulyawan, A., Sarwanto, Y., … Taryana, Y. (2019). Metamaterial: Smart Magnetic Material for Microwave Absorbing Material. In K. H. Yeap & K. Hirasawa (Eds.), *Electromagnetic Fields and Waves* (pp. 1–18). IntechOpen. https://doi.org/10.5772/intechopen.84471

Akmal Johan, Wisnu Ari Adi, F. S. A. and D. S. (2019). Analysis crystal structure of magnetic materials Co1-xZnxFe2O4. *Journal of Physics: Conf. Series*.

C. G. Sun, H. J. L. Li Taoa, C. J. Huang, H. S. Z. and Z. S. C. (2006). Preparation and characterization of hexagonal mesoporous titanium–cobalt oxides. *Materials Letters*, *60*(17–18), 2115–2118.

Chu, X., Liu, X., Wang, G., & Meng, G. (1999). Preparation and gas-sensing properties of nano-CoTiO3. *Materials Research Bulletin*. https://doi.org/10.1016/S0025-5408(99)00167-1

Emery, W & Camps, A. (2017). *Introduction to Satellite Remote Sensing*. Amsterdam: Elsevier.

Folgueras, L. de C., Alves, M. A., & Rezende, M. C. (2010). Microwave absorbing paints and sheets based on carbonyl iron and polyaniline: Measurement and simulation of their properties. *Journal of Aerospace Technology and Management*. https://doi.org/10.5028/jatm.2010.02016370

Gunanto, Y. E., Jobiliong, E., & Adi, W. A. (2016). Microwave absorbing properties of Ba0.6Sr0.4Fe12-zMnzO19(z = 0-3) materials in

XBand frequencies. *Journal of Mathematical and Fundamental Sciences*. https://doi.org/10.5614/j.math.fund.sci.2016.48.1.6

He., H. Y. (2007). Humidity sensitivity of CoTiO3 thin film prepared by sol–gel method. *Materials Technology*, *22*(2), 95–97.

Keerthana, K., Shanmugha Sundaram, G. A., & Soman, K. P. (2018). Effect of jammer signal on stepped frequency PAM4 radar waveforms. In *Procedia Computer Science*. https://doi.org/10.1016/j.procs.2018.10.347

Khalil, A., & Celik, K. (2019). Optimizing reactivity of light-burned magnesia through mechanical milling. *Ceramics International*. https://doi.org/10.1016/j.ceramint.2019.07.324

Kumar, S., Supriya, S., Pradhan, L. K., & Kar, M. (2017). Effect of microstructure on electrical properties of Li and Cr substituted nickel oxide. *Journal of Materials Science: Materials in Electronics*. https://doi.org/10.1007/s10854-017-7580-4

Lee, D., Choi, I., & Lee, D. G. (2015). Development of a damage tolerant structure for nano-composite radar absorbing structures. *Composite Structures*. https://doi.org/10.1016/j.compstruct.2014.08.001

Lenin, N., Sakthipandi, K., Kanna, R. R., & Rajesh, J. (2018). Effect of neodymium ion on the structural, electrical and magnetic properties of nanocrystalline nickel ferrites. *Ceramics International*. https://doi.org/10.1016/j.ceramint.2018.03.218

Li, M. W., Gao, X. M., Hou, Y. L., & Wang, C. Y. (2013). Characterization of CoTiO3 nanocrystallites prepared by homogeneous precipitation method. *Journal of Nano- and Electronic Physics*.

Li, W., Lina, L., Lia, C., Wang, Y., & Zhang, J. (2019). Radar absorbing combinatorial metamaterial based on silicon carbide/ carbon foam material embedded with split square ring metal. *Results in Physics*, *12*, 278–286.

Li, X. M., Luo, D., Qiu, C. Y., & Li, C. (2011). Adaptive generalized DPCA algorithm for clutter suppression in airborne radar system. In *Proceedings of 2011 IEEE CIE International Conference on Radar, RADAR 2011*. https://doi.org/10.1109/CIE-Radar.2011.6159743

Liu, J. R., Itoh, M., Horikawa, T., Itakura, M., Kuwano, N., & Machida, K. I. (2004). Complex permittivity, permeability and electromagnetic wave absorption of α-Fe/C(amorphous) and Fe2B/C(amorphous) nanocomposites. *Journal of Physics D: Applied Physics*. https://doi.org/10.1088/0022-3727/37/19/019

Panwar, R., Agarwala, V., & Singh, D. (2015). A cost effective solution for development of broadband radar absorbing material using electronic waste. *Ceramics International*. https://doi.org/10.1016/j.ceramint.2014.10.118

Phan, T. L., Zhang, P., Grinting, D., Yu, S. C., Nghia, N. X., Dang, N. V., & Lam, V. D. (2012). Influences of annealing temperature on structural characterization and magnetic properties of Mn-doped BaTiO 3 ceramics. *Journal of Applied Physics*. https://doi.org/10.1063/1.4733691

R. E. Newnham, J. H. F. and R. P. S. (1964). Crystal structure and magnetic properties of CoTiO3. *Acta Crystallographica*, *17*(3), 240–242.

Sarkar, B., Pendem, C., Konathala, L. N. S., Sasaki, T., & Bal, R. (2014). Formation of ilmenite-type CoTiO3 on TiO2 and its performance in

oxidative dehydrogenation of cyclohexane with molecular oxygen. *Catalysis Communications*. https://doi.org/10.1016/j.catcom.2014.06.021

Schoofs, F., Egilmez, M., Fix, T., MacManus-Driscoll, J. L., & Blamire, M. G. (2013). Structural and magnetic properties of CoTiO3 thin films on SrTiO3 (001). *Journal of Magnetism and Magnetic Materials*. https://doi.org/10.1016/j.jmmm.2012.12.017

Shiva, A. V. N. R. S., Elleithy, K., & Abdelfattah, E. (2017). Improved monostatic pulse radar design using ultra wide band for range estimation. In *2016 Annual Connecticut Conference on Industrial Electronics, Technology and Automation, CT-IETA 2016*. https://doi.org/10.1109/CT-IETA.2016.7868245

Siemons, M., & Simon, U. (2007). Gas sensing properties of volume-doped CoTiO3 synthesized via polyol method. *Sensors and Actuators, B: Chemical*. https://doi.org/10.1016/j.snb.2007.04.009

Silva, R. A., Oliveira, R. G. M., Silva, M. A. S., & Sombra, A. S. B. (2019). Effect of V2O5 addition on the structural and electrical properties of CoTio3. *Composites Part B: Engineering*. https://doi.org/10.1016/j.compositesb.2019.107286

Vinogradov, A. V., Vinogradov, V. V., Gerasimova, T. V., & Agafonov, A. V. (2012). Low-temperature sol-gel synthesis of crystalline CoTiO3 coatings without annealing. *Journal of Alloys and Compounds*. https://doi.org/10.1016/j.jallcom.2012.06.102

Wang, S. Q., Hu, G. P., Zhang, Q. L., Gao, C. Y., & Cai, T. (2018). The Background and Significance of Radar Signal Sorting Research in Modern Warfare. In *Procedia Computer Science*. https://doi.org/10.1016/j.procs.2019.06.080

Wu, C., Chen, S., Gu, X., Hu, R., Zhong, S., Tan, G., … Li, R. W. (2018). Enhanced and broadband absorber with surface pattern design for X-Band. *Current Applied Physics*. https://doi.org/10.1016/j.cap.2017.10.012

Yadav, B. C., Yadav, R. C., Singh, S., Dwivedi, P. K., Ryu, H., & Kang, S. (2013). Nanostructured cobalt oxide and cobalt titanate thin films as optical humidity sensor: A new approach. *Optics and Laser Technology*. https://doi.org/10.1016/j.optlastec.2012.12.011

Yang, G., Yan, W., Wang, J., & Yang, H. (2014). Fabrication and characterization of CoTiO3 nanofibers by sol-gel assisted electrospinning. *Materials Letters*. https://doi.org/10.1016/j.matlet.2014.01.177

Zou, J., & Zheng, W. (2016). TiO2@CoTiO3 complex green pigments with low cobalt content and tunable color properties. *Ceramics International*. https://doi.org/10.1016/j.ceramint.2016.02.029

Zwinkels, J. (2015). Light, Electromagnetic Spectrum. In L. R (Ed.), *Encyclopedia of Color Science and Technology* (pp. 1–8). Berlin, Heidelberg: Springer. https://doi.org/https://doi.org/10.1007/978-3-642-27851-8_204-1